

Supplement

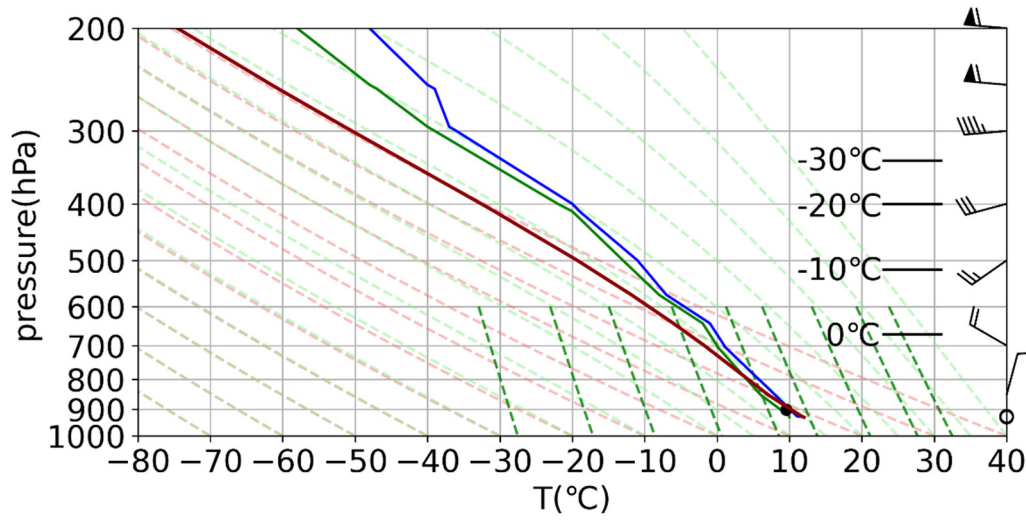


Figure S1: Radiosonde at 08:00 (BJT) on September 26th, 2017.

5

10

15

20

25

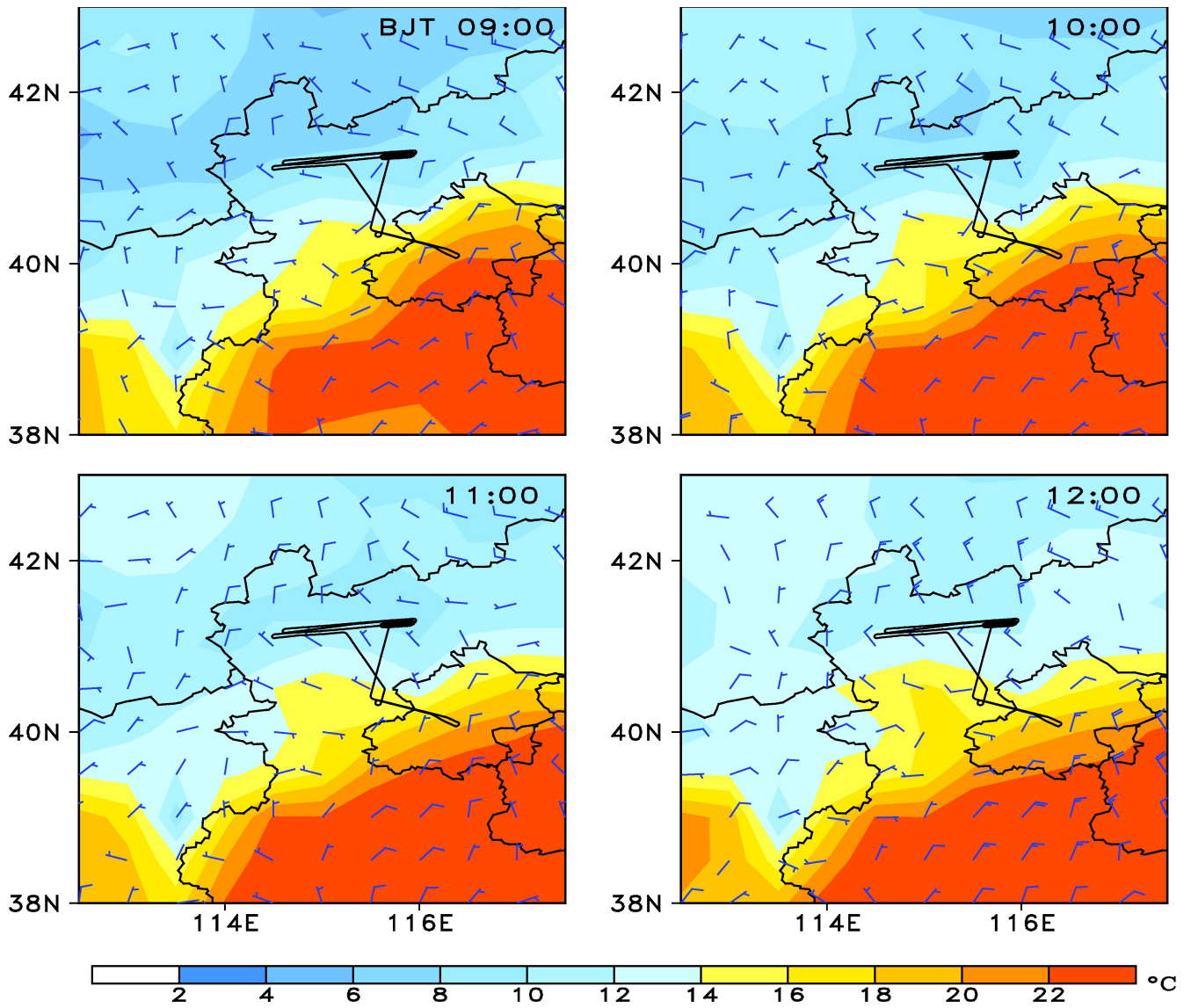
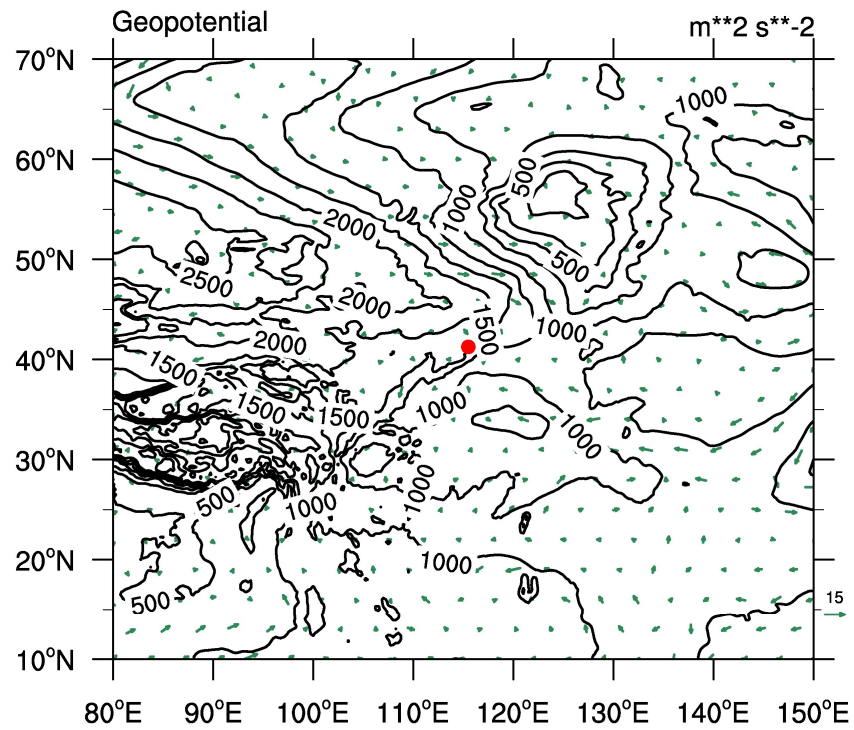


Figure S2: Flight tracks (black line) mapping on the wind field (blue wind shaft) and temperature field (color) observed by ground weather observation station at 09:00-12:00 (BJT) on September 26th, 2017.



35 **Figure S3: Geopotential height contour map at 1000 hPa at 09:00 (BJT) on September 26th, 2017. The experimental region is indicated by the red dot.**

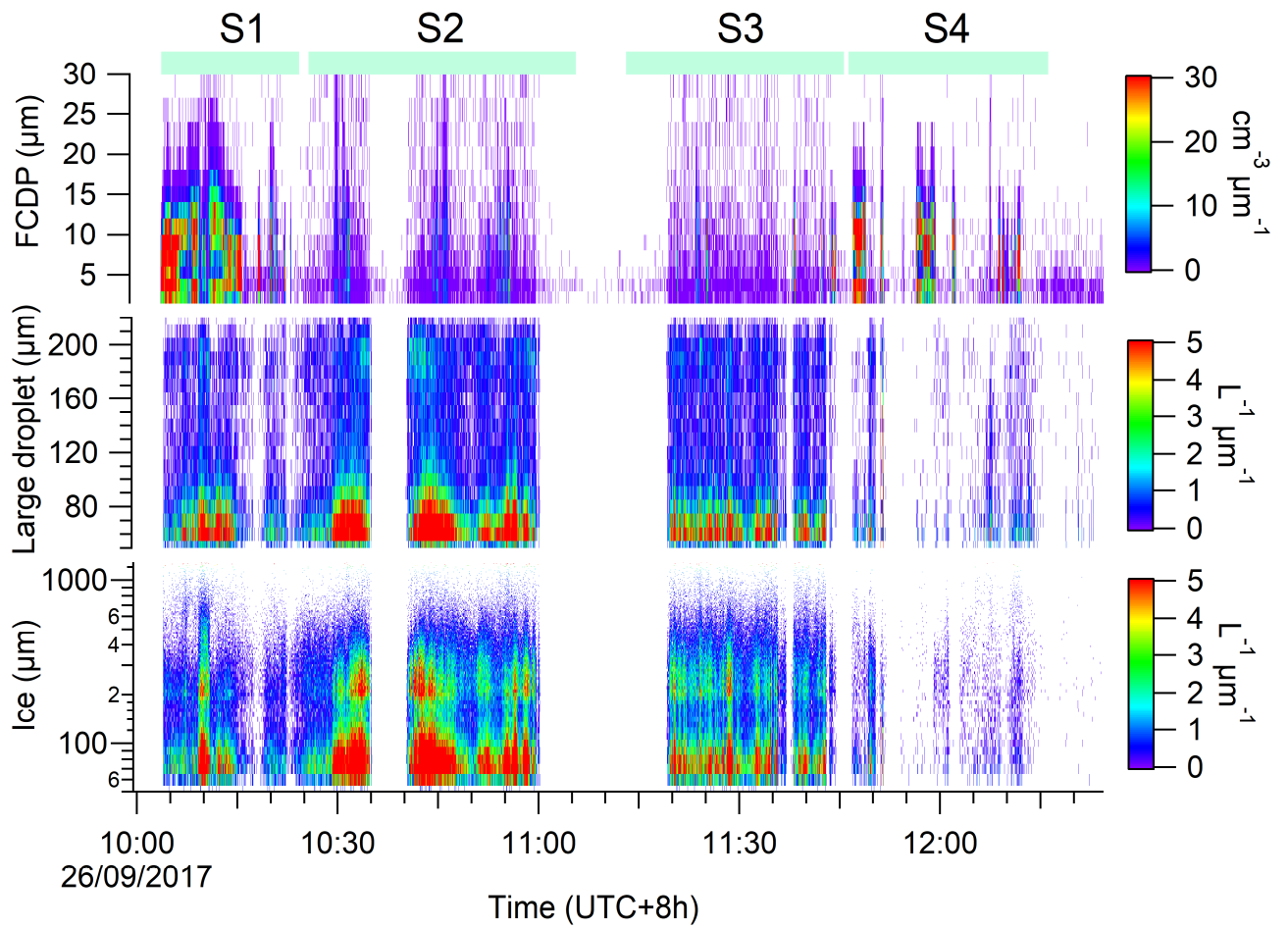


Figure S4: Particle size distribution spectrum of FCDP and 2D-S (ice and large droplet).

40

45

50

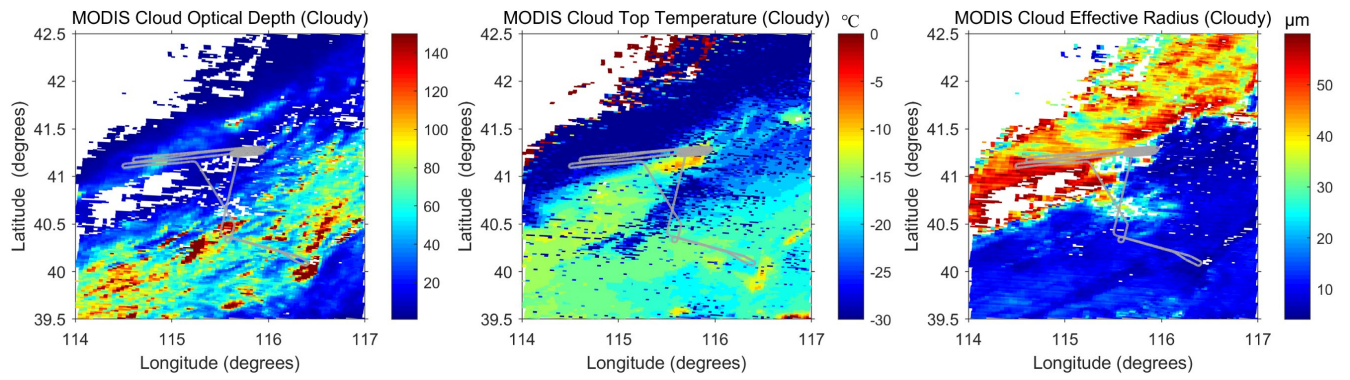


Figure S5: Cloud optical depth, cloud-top temperature and cloud effective radius from MODIS at 10:30 (UTC+8h) on September 26th, 2017, with flight track shown in grey line.

55

60

65

70

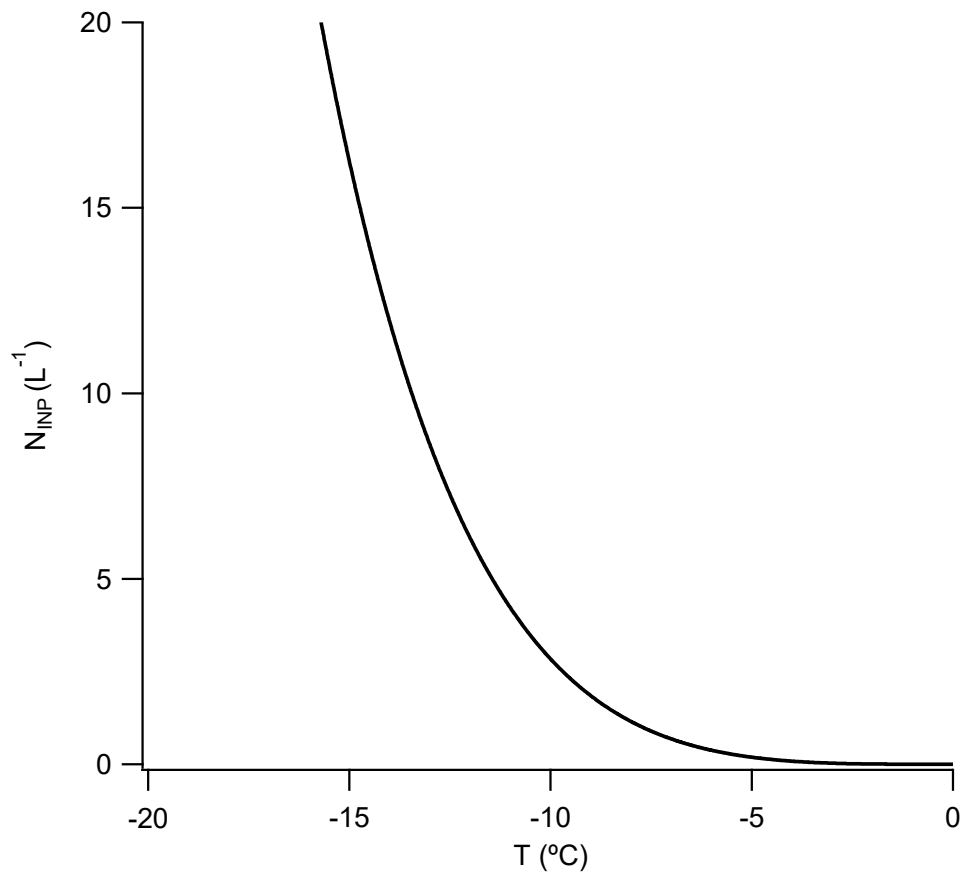
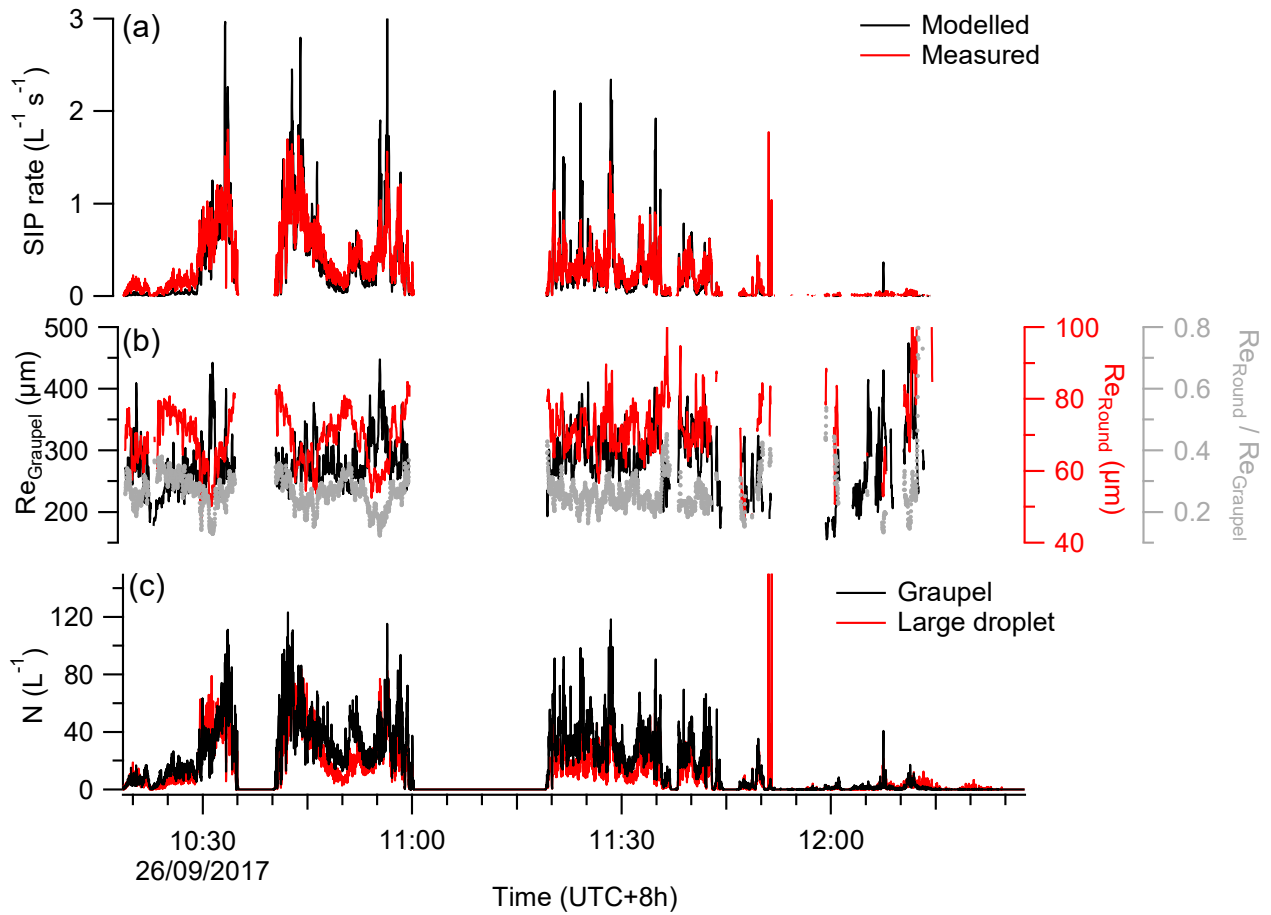
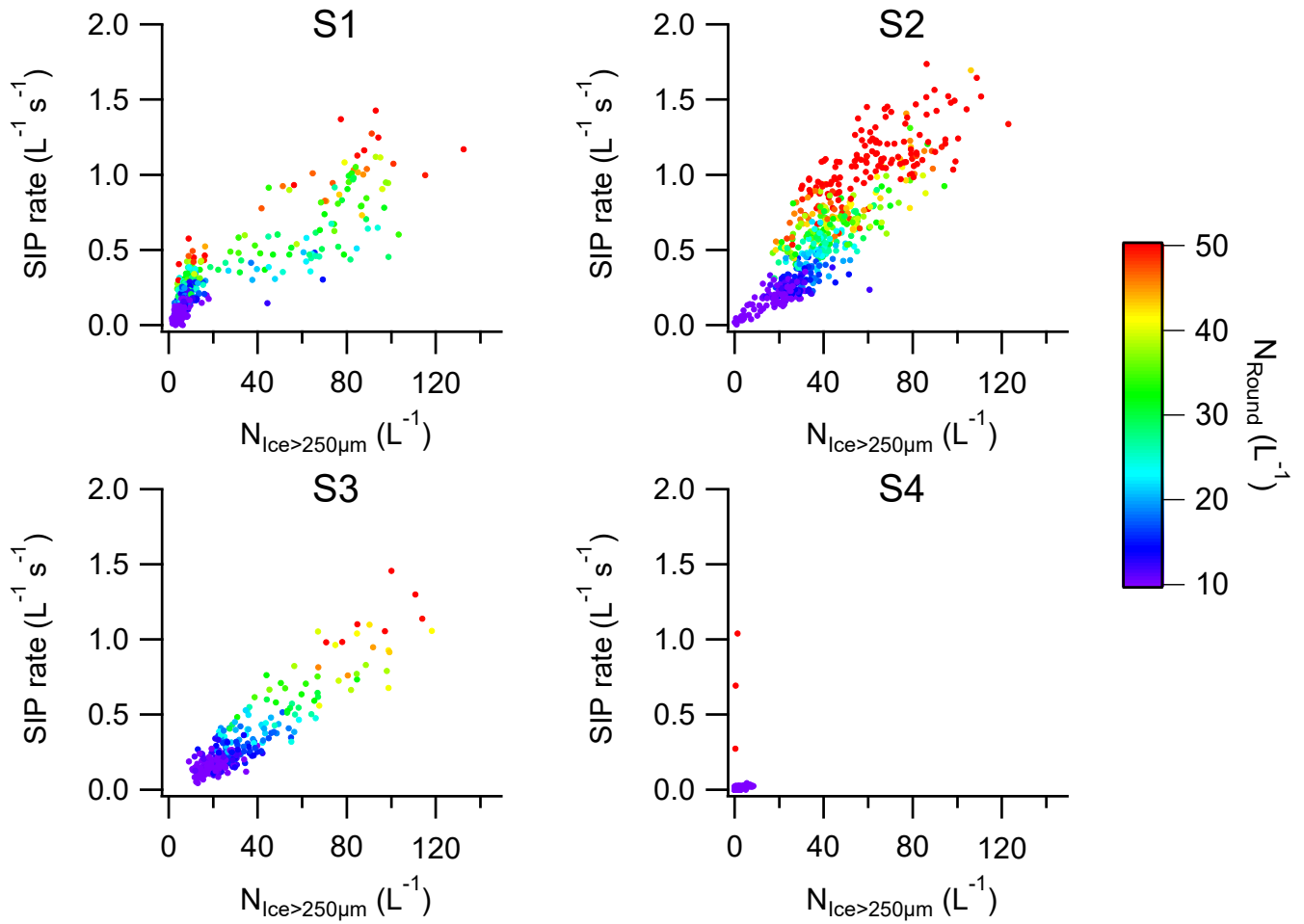


Figure S6: The number concentration of ice nucleating particles (N_{INP}) as a function of cloud temperature, taking into account a 10-fold error.



75

Figure S7: Time series of modelled and measured secondary ice production (SIP) rate. (a) The modelled and measured SIP rate, (b) Effective radius of graupel ($Re_{Graupel}$) and large droplet (Re_{Round}), and the ratio between its ($Re_{Round} / Re_{Graupel}$), (c) Number concentrations (N) of graupel and large droplet.



80 **Figure S8:** The number concentration of ice with diameter $> 250 \mu m$ ($N_{Ice>250\mu m}$) as a function of the measured SIP rate at different stages, colored by N_{Round} .